T.C.
FATIH UNIVERSITY
INSTITUTE OF BIOMEDICAL ENGINEERING

**OPTICAL CHARACTERIZATION OF CANCEROUS AND
CORRESPONDING HEALTHY TISSUE SAMPLES WITH DOUBLE
INTEGRATING SPHERE SYSTEM**

VOLKAN DİNÇ

MSc THESIS
BIOMEDICAL ENGINEERING PROGRAMME

i

İSTANBUL, JUNE 2013

T.C.
FATIH UNIVERSITY
INSTITUTE OF BIOMEDICAL ENGINEERING

OPTICAL CHARACTERIZATION OF CANCEROUS AND CORRESPONDING HEALTHY TISSUE SAMPLES WITH DOUBLE INTEGRATING SPHERE SYSTEM

VOLKAN DİNÇ

MSc THESIS
BIOMEDICAL ENGINEERING PROGRAMME

İSTANBUL, JUNE 2013

T.C.
FATIH ÜNİVERSİTESİ
BİYOMEDİKAL MÜHENDİSLİK ENSTİTÜSÜ

SAĞLIKLI VE KANSERLİ DOKULARIN ÇİFT TOPLAYICI KÜRE SİSTEMİ İLE OPTİK ÖZELLİKLERİNİN İNCELENMESİ

VOLKAN DİNÇ

YÜKSEK LİSANS TEZİ
BİYOMEDİKAL MÜHENDİSLİK PROGRAMI

DANIŞMAN
YARD. DOÇ. HAŞİM ÖZGÜR TABAKOĞLU

iii

İSTANBUL, HAZİRAN 2013

T.C.
FATIH UNIVERSITY
INSTITUTE OF BIOMEDICAL ENGINEERING

Volkan Dinç, a **MSc.** student of Fatih University **Institute of Biomedical Engineering** student ID **52011002**, successfully defended the **thesis/dissertation** entitled "**OPTICAL CHARACTERIZATION OF CANCEROUS AND CORRESPONDING HEALTHY TISSUE SAMPLES WITH DOUBLE INTEGRATING SPHERE SYSTEM**", which he prepared after fulfilling the requirements specified in the associated legislations, before the jury whose signatures are below.

Thesis Advisor : Asst.Prof. Haşim Özgür Tabakoğlu
Fatih University

Jury Members : Asst.Prof. Saime Akdemir Akar
Fatih University

Asst.Prof. Kadir Tufan
Fatih University

Date of Submission: 17 May 2013
Date of Defense :   21 June 2013

To my father, who believed in me when no one else did

Special thanks to Gamze Bölükbaşı, Oğuzhan Karatepe, Tuğba Kiriş, Ayşenur Kiriş and Saadet Akbulut for making everything easier

ACKNOWLEDGEMENTS

I'd like to thank to my thesis advisor Assit.Prof.Haşim Özgür Tabakoğlu for his unique suggestions, unlimited help, and endless support for all along this study and my master programme, and also I want to thank to him for being more than just a teacher to me..

I'd like to thank to Yrd.Doç Saime Akdemir Akar for being a member for my thesis committee and for her precious observations and suggestions

I'd like to thank to Yrd.Doç. Kadir Tufan for being a member for my thesis committee and for his precious observations and suggestions

Special thanks to:

Dr. Oğuzhan Karatepe for making it possible for us to get the tissues we need

Gamze Bölükbaşı for teaching me how to use the DIS system and answerin all my questions even in the middle of the night

Saader Akbulut, Tuğba Kiriş, Ayşenur Kiriş for taking care of the tissues and made the tissues delivered to me no matter what the day and time is

And very special thanks to Prof.Dr.Sadık Kara for letting me learn things I want to learn in Fatih University

June 2013   Volkan Dinç

TABLE OF CONTENTS

LIST OF SYMBOLS

G   Anisotropy factor

$I_{in}(\eta c)$ The reflection redistribution

$T(\eta'c, \eta c)$ Transmission redistribution function

E   The identity matrix

w_i The weight assigned to the ith quadrature point

δ_{ij} Kroneker delta symbol

ABBREVIATIONS

IAD   : Inverse Adding Doubling
DIS   : Double Integrating Sphere
PDT   : Photo Dynamic Therapy
LCD   : Liquid Crystal Display
MUA   : Absorption Coefficient
MUS   : Scattering Coefficient
NM   : Nanometer

LIST OF FIGURES

LIST OF TABLES

SUMMARY

OPTICAL CHARACTERIZATION OF CANCEROUS AND CORRESPONDING HEALTHY TISSUE SAMPLES WITH DOUBLE INTEGRATING SPHERE SYSTEM

Volkan DİNÇ

Biomedical Engineering Programme

MSc Thesis

Advisor: Assist.Prof. Haşim Özgür Tabakoğlu

Aim of this study is to measure the optical properties of both *ex-vivo* cancerous tissue samples and normal, healthy tissue samples. Results have been compared to observe how cancerous and noncancerous tissues behave in visible spectrum, between 550 nm and 650 nm. *Ex-Vivo* tissue samples have been obtained from Bezmialem Hospital. Optical characterization has been performed in Medical Laser Laboratory at Boğaziçi University, Biomedical Engineering Institute.

Tissue optical properties have been measured by using a Double Integrating Sphere system and some computational techniques like Inverse Adding Doubling Method (IAD). With IAD simulation technique, accurate estimates of optical properties like scattering, reflection and absorption, for biological tissues can be observed. By doing so, pathological results have been tried to be estimated without using histological staining methods and has been tried to be developed new methods and techniques for pathologic assessments to help surgeons and pathologists during surgical operation.

Keywords: Double Intergrating Sphere, monochromator, absorption, scattering, pathology

FATIH UNIVERSITY - INSTITUTE OF BIOMEDICAL ENGINEERING

ÖZET

SAĞLIKLI VE KANSERLİ DOKULARIN ÇİFT TOPLAYICI KÜRE SİSTEMİ İLE OPTİK ÖZELLİKLERİNİN İNCELENMESİ

Volkan DİNÇ

Biyomedikal Mühendislik Programı

Yüksek Lisans Tezi

Danışman: Yard. Doç. Haşim Özgür TABAKOĞLU

Bu çalışmanın amacı ex-vivo olarak hem kanserli hem de sağlıklı dokuların optik özelliklerini ölçmektir. Sonuçlar, kanserli ve kanserli olmayan dokuların görünür bölgede 500nm ve 650nm arasında nasıl danvrandığını incelemek adına karşılaştırılacaktır. Ex-Vivo doku örnekleri Bezmialem Hastanesi'nden elde edilmiştir. Optik karakteristik incelemeleri ise Boğaziçi Üniversitesi Biyomedikal Mühendislik Enstitüsü'ndeki Medikal Lazer Laboratuar'ında yapılmıştır.

Dokuların optik özellikleri Çift Toplayıcılı Küre sistemi ve Inverse Adding Doubling (IAD) metodu gibi bilgisayar programları ile yapılmıştır. IAD simülasyon tekniği ile biyolojik dokuların, saçılma, yansıma ve absorbe olmaları gibi optik özellikler incelenebilmektedir. Bunu yaparak da patolojik sonuçların tahmini, boyama gibi histolojik yöntemler olmadan yapılmaya çalışılmıştır ve doktorlara ve patolojicilere ameliyatlar sırasında yeni metodlar ve teknikler üretilmeye çalışılmıştır.

Anahtar kelimeler: Çift toplayıcılı küre, monokromatör, absorbsiyon, saçılma, patoloji

FATİH ÜNİVERSİTESİ -BİYOMEDİKAL MÜHENDİSLİK ENSTİTÜSÜ

CHAPTER 1

INTRODUCTION

1.1 Literature Survey

An accurate or probable estimation of optical properties of tissues has been of great interest for many years and subject for research from various disciplines like physics, medicine, chemistry and biomedical engineering. Double Integrating Sphere system and both Inverse Adding Doubling Method and Inverse Monte Carlo Method have been widely used methods in order to measure the optical properties of the tissues [1].
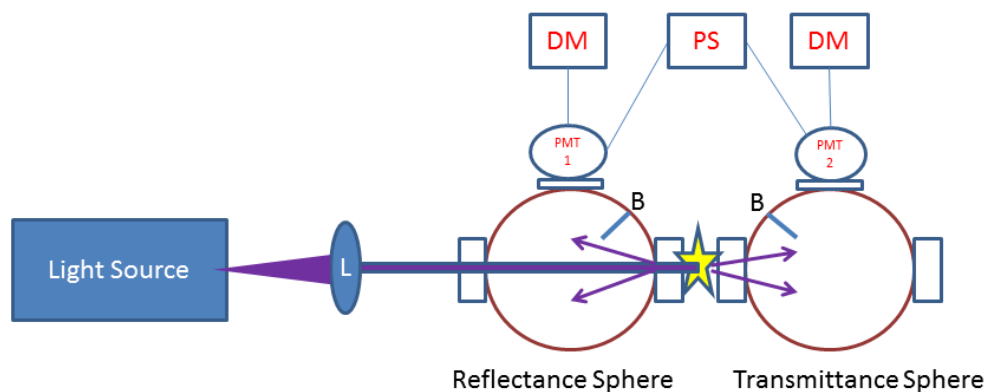
Figure 1.1. Double Integrating Sphere System with monochromator. Star represents tissue. DM=Digital multimeter, PS=Power source, PMT=Photomultiplier tube, B:Baffle, L: Lens. Reproduced From Sardar *et al* [1]

Inverse Monte Carlo Method (IMC) is used as photon distribution and for simulation of random processes the Monte Carlo (MC) Method could be preferred. The MC method is based on Law Of Large Numbers and Central Limit Theorem [2]. The MC method gives chance to calculate some impractical distributions. It basically 'guesses' the outcome of an equation. The IMC calculations include the direct solution, a forward MC calculation, sphere geometrical parameters, the optical properties of the media and the inverse solution that determines a minimum by iteration [3].

The measured optical properties have been run on different calculation methods (like Kubelka Munk or IMC etc) to make a comparison and for verifying the coefficients like absorption and scattering.

Healthy and unhealthy values *in vitro* have been measured for Photodynamic Therapy (PDT) purposes [4]. In addition light delivery information has been gained for PDT treatment.

By taking advantages of optical property measurements [4], researchers decided that there were no significant differences between the normal and adenomatous samples of the same tissue but there were significant differences between the different types of tissues so researchers decided that the structure of these tissues had to be significantly different.

The best description of optics for laser irradiation was the examination of the response of a target within tissue to light. Suppose there was a chromophre like a melanocyte at coordinate r(x,y,z) inside the tissue.

There had to be photon propagation in this tissue if light was interacted with it, and in that case the characteristics of this propagation like scattering and absorption must have governed the number of photons that would reach the melanocyte at the coordinate r. In this example scattering was an important matter for it could changed the direction of propagation of a photon in both forward and backward direction and besides most of the photons never hit the melanocyte. Also these photons could be absorbed by other tissue chromophores; also these photons could be remitted out of the tissue and/or reflected [5,6].
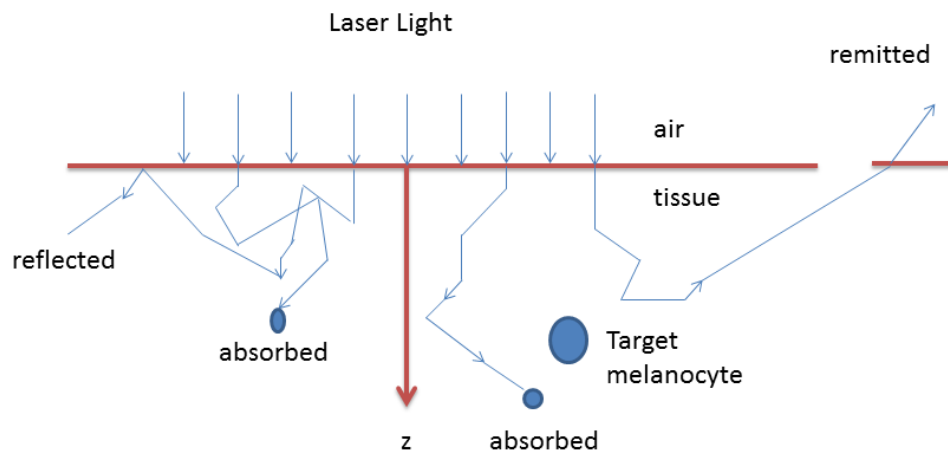
Figure 1.2 Photon Propagation in The Tissue. Reproduced from Martian *et al* [5]

In this study the tissues, which would be examined, were cancerous and non-cancerous tissue samples, so some general information about cancer and its optical properties could be explained in detail in next sections.

Cancer might be defined as a progressive series of genetic events which occured in a single clone of cells because of some alterations in vey limited number of specific genes like oncogenes and tumor suppresor genes [7-9]. Cancers also might be known as malignant neoplasm where the word of neoplasm came from ancient Greek and ment abnormal mass of tissue (neo means new and plasma means formation and creation) [10].

All of the cancers were involved unregulated cell growth. Where a cancer begun to grow, the cells divided and growth uncontrollably, formed tumors and invaded surrounding tissues of the body [11]. Some cancers could also spread to more distant

parts of the body through the lymphatic system or bloodstream and made metastase. At this point it has to be said that not all of cancers are cancerous [12]. These non-cancerous tumors are called benign tumors, which do not grow uncontrollably like malignant tumors [13]. Detarmanitaion of the causes of the cancer is very complex. There are many methods, which are clinically used for the diagnosis and the treatment of the cancer. One of these methods is light based therapies and diagnosis. The knowledge of the behavior of the light in specific cancerous tissues is very important because the therapatic aspects of the cancerous tissues mainly depend on the amount of the absorbed light and scattered light [14-17]. At this very point the depth and the thickness of the cancerous tissue was important too. Also, the optical properties of cancerous tissues is a highly important phenomenon for the light based diagnosis and treatment of the cancer because every specific tissue (e.g lung, breast, pancreas etc.) changes its structural and physiological properties when it became cancerous therefore its optical characteristis changes too. So, every interaction with light of every specific tissue (its absorption and scattering coefficients) are vary and different from each other. And this is why it is a key factor to know that how a specific tissue behaves to a specific wavelength [18-23].

1.2   Purpose of the Thesis

With the upcoming technology new kind of research areas has emerged. One of these areas is measurement of the optical properties of tissue. In recent years there has been considerable interest in these measurements and their accuracy. These measurements include scattering, reflection and absorption coefficients. These properties have been measured by using a Double Integrating Sphere system. These optical properties are fundamental optical properties of biological tissues and can be used for the diagnosis of various diseases. The quantitative distribution of light intensity in biological media can be obtained from radiative transport equation [24, 25]:

$$\frac{dI(r,s)}{ds} = -(\mu_a + \mu_s)I(r,s) + \frac{\mu_s}{4\pi} \int_{4\pi} p(s,s')I(r,s')d\Omega' \qquad \text{[Eqn 1]}$$

An analytical solution to this equation is very hard to achieve beacause of the complexity of the nature of biological media and because of their irregular shapes. However, Prahl *et al* found a logical solution to solve the transport equation, which is known as Inverse Adding Doubling (IAD) [26].

In this study, the Double Integrating Sphere system had been used to measure the optical properties of tissues and method of Inverse Adding Doubling had been used to evaluate these optical properties. With IAD simulation technique, more accurate estimates of optical properties could be got; like scattering, reflection and absorption, for biological tissues. In regards to these, the aim of this study is to measure the optical properties of both cancerous tissue samples and normal, healthy (non-cancerous) tissue samples. By doing that we will try to *estimate* pathological results without using staining methods and try to develop new methods and techniques for pathologic assessments to help surgeons and pathologists during surgical operation.

1.3   Hypothesis

The hypothesis of this study is to show that the optical charecteristics of cancerous and normal tissues are different. When a cell becomes cancerous it changes in every aspect. Every characteristic of the tissue change and therefore becomes completely different from a healthy cell. And thus, the interaction with light for cancerous and healthy cells 'has' to be different. Our hypothesis here is to prove that optical charecteristics of cancerous and healthy tissues are different and so this way, somehow help both medical imaging and treatment aspect of this science. And make it a little bit easier for both patients with cancer and doctors who tries to treat them in a correct way by providing useful information about cancer diagnosis and treatment.

1.4 Motivation

The motivation of this study and the answer of the question 'why we did such a study?' and 'what drives us?' can be summarized to one sentence at all: *We wanted to help the diagnosis and the treating aspects of cancer*. We can simply hope that what we ***tried*** to do here will help developing more innovative technologies for patiens, doctors and scientist around the world who has a crossway with cancer in their lifes.

CHAPTER 2

MATERIAL AND METHOD

All the experiments have been conducted under permission of Fatih University Medical Faculty. (Ethical commision report for clinical researches Number: B 30 2 FTH 0 20 00 00 / 0730)

As a preliminary study, a lamb kidney tissue that was bought from a local slaughterhouse has been practiced with DIS in order to optimize measurement procedures. After the system stabilized, tissue samples (preserved in PBS solution) taken from hospital have been homogenized. Homogenized samples were put in between slides that distance is known. Measurements were taken with DIS. Specteral range for the study in between 400nm and 700nm was selected and performed in this range, which is the visible region.

The tissue samples for all experiments have been obtained from Bezmi Âlem Hospital and all of the tissue optical characterization experiments have been perfomed in Medical Lasers Laboratory at Boğaziçi University, Institute of Biomedical Engineering.

2.1 Experimental Set up Of Double Integrating Sphere

The main components of the system are described in the order of path followed by light: light source, lens 1, monochromator, chopper, lens 2, spheres, a lock-in amplifier. The light source is the source for the light, which comes out of the monochromator and gets into the spheres.

Figure 2.1 The light source (Mille Luce M 1000)

A monochromator is an optical device that transmits a mechanically selectable narrow band of wavelengths of light or other radiation chosen from a wider range of wavelengths available at the input.

Although some monochromator designs do use focusing gratings that do not need separate collimators, most use collimating mirrors. Reflective optics is preferred because they do not introduce dispersive effects of their own [27]. In our system set two lenses were put in two sides of the monochromator in purpose of gathering the incoming light and focus it. The first lens was put in between the light source and the monochromator and the second lens was put in between the monochromator and DIS system. The monochromator was connected to a desktop PC and controlled by a programme, which was run on the PC. The desired wavelengths and the increasment between the wavelength scan steps were adjustable because of this programme on the PC.
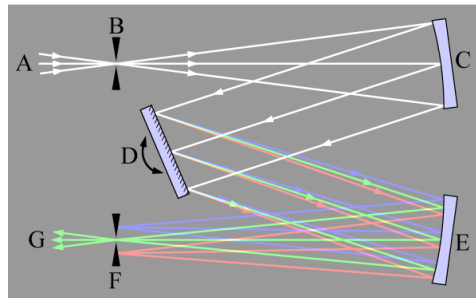
Figure 2.2 Diagram of a monochromator [27]

Figure 2.3 The monochromator (CVI DK 480 ½ meter)

A chopper circuit is used to refer to numerous types of electronic switching devices and circuits. Essentially, a chopper is an electronic switch that is used to interrupt one signal under the control of another.

Figure 2.4 The chopper used for our study (Stanford Research Systems SR540)

Double Integrating Sphere System used in this study was shown below (Figure 2.5). An integrating sphere system is a system, which consists of a hollow spherical cavity that has an inner surface that is covered by a diffuse white reflective coating as well as with small entrance and exit portholes. Its characteristic is that it is a uniformscattering or diffusing effect. Any light rays that collide with the inner surface are by multiple scattering reflections and distributed equally to all other points. The actual directions of light's effects are minimized. The system could be thought of as a diffuser that destroys spatial information but preserves power. It has a baffle inside near to the sample area which prevents the first reflection and scattered light collected by a dedector because the system primerly prefers the light to diffuse inside the sphere not come to the dedector directly [28,29].

Figure 2.5: The Double Integrating Sphere System at Boğaziçi University, Institute of Biomedical Engineering (Labsphere General Purpose sphere, spectralon, 4 ports-033 inch diameter)

A lock-in amplifier (also known as a phase-sensitive detector) is a type of amplifier that can extract a signal with a known carrier wave from an extremely noisy environment (the signal-to-noise ratio can be -60 dB or even less). It is essentially a homodyne detector followed by a steep low pass filter, making it very narrow band. Practical lock-in amplifiers use mixing, through a frequency mixer, to convert the signal's phase and amplitude to a DC — actually a time varying low frequency — voltage signal [30].
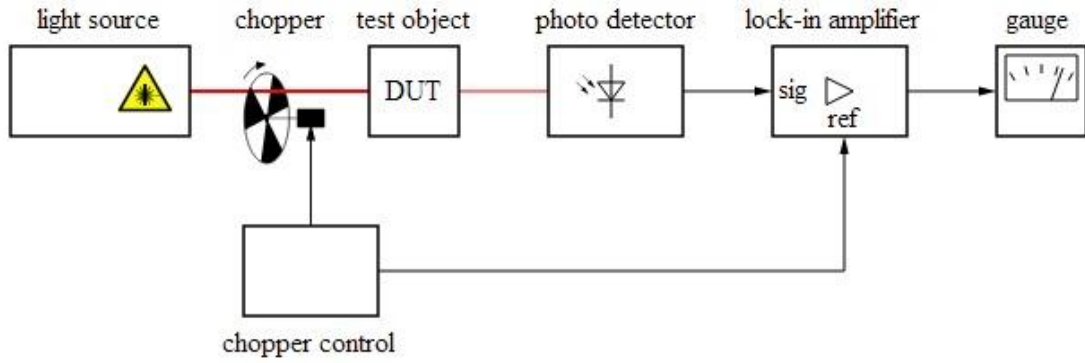
Figure 2.6 Experimental set up of a lock-in amplifier

Figure 2.7 The lock-in amplifier used in our study (Stanford Research Systems, SR510)

The computer system connected can be seen in the picture 2.3 above. And the sphere system was explained in detail in the Introduction. The only thing remains at this point that need to be explained the simulation programme that was in used in this study.

Prahl's Inverse Adding Doubling simulation programme was used in this study.

In the name of using Prahl's IAD simulation programme, we calculated the reflectance (MR) and transmittance (MT) values for these are the parameters needed to use the programme. These values were calculated by two different formulas, which are indicated below:

$$M_R = r_{std} \frac{R_2\left(r_s^{\,direct}, r_s, t_s^{\,direct}, t_s\right) - R_2(0,0,0,0)}{R_2(r_{std}, r_{std}, 0,0) - R_2(0,0,0,0)}$$

[Eqn. 2]

And

$$M_T = \frac{T_2(r_s^{\,direct}, r_s, t_s^{\,direct}, t_s) - T_2(0,0,0,0)}{T_2(0,0,1,1) - T_2(0,0,0,0)}$$

[Eqn. 3]

Also, to use Prahls's IAD one needs anisotropy factor [which was accepted as 0.9 in biological tissues (g=0.9)], refractive index of soft tissues (which was accepted as 1.34),

9

refractive index of the thickness of the sample, thickness of the slides, and diameter of the entries. These informations were mostly taken from the literature except reflectance and transmittance values and the thickness of the slides. To measure our specific reflectance and transmittance values; five different measurements must be made and each of them must be repeated three times for optimizing the standard deviation of the system [26]

$$R_2(r_s^{direct}, r_s, t_s^{direct}, t_s) \quad T_2(r_s^{direct}, r_s, t_s^{direct}, t_s)$$

$$R_2(r_{std}, r_{std}, 0, 0) \quad T_2(0, 0, 1, 1)$$

$$R_2(0, 0, 0, 0) \quad T_2(0, 0, 0, 0)$$
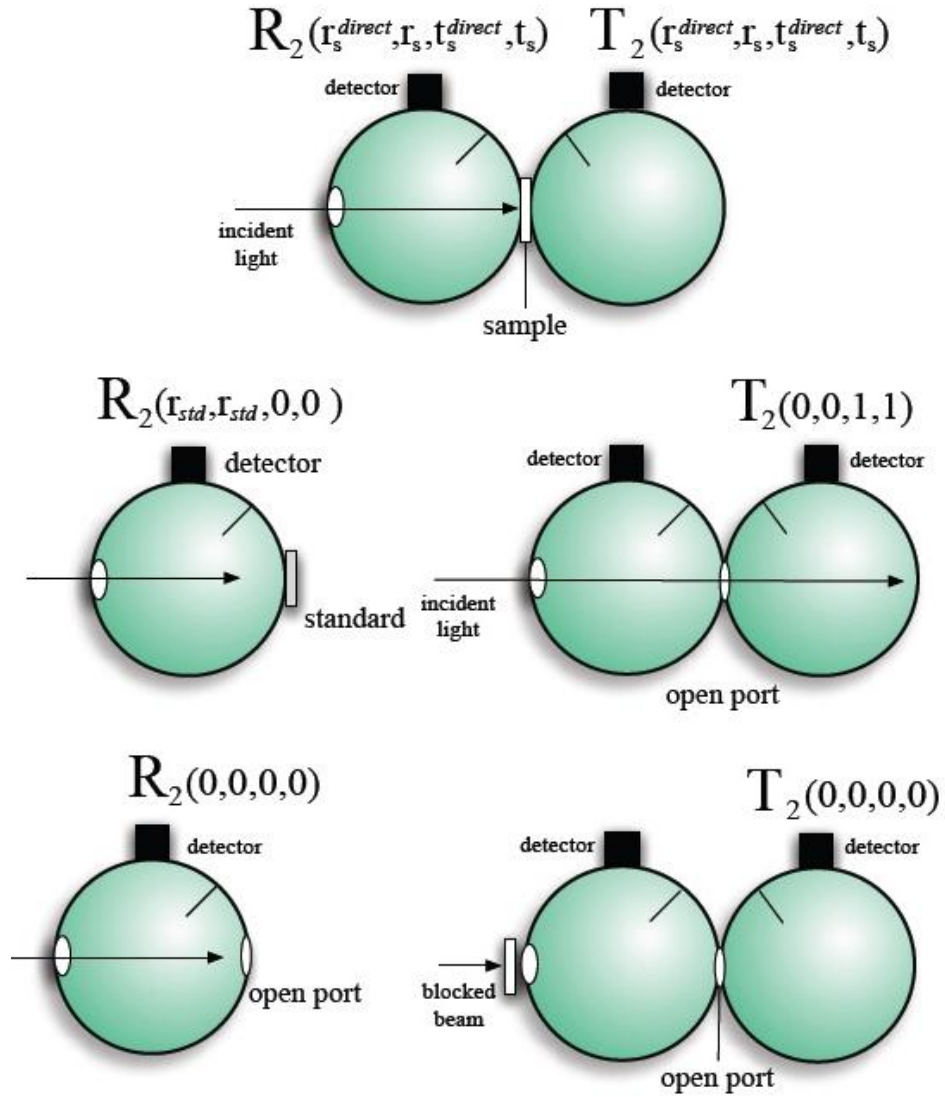
Figure 2.8: The diagram for different measurements which are used to calculate MR and MT by DIS System

In the first measurement, the reflectance standard, which is 99% reflector, was put on the exit of reflectance sphere.

10
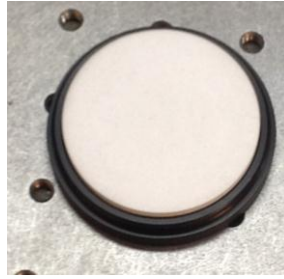
Figure 2.9 The Reflectance Standard

The incoming light collides that named as standard and scatters. Some part of the entire light have been totally reflected from the standard and got out from the way it exactly came in. But the remaining beams have been scattered all over the inner surface of the Reflectance Sphere and eventually collected by the dedector. With this type of measurement the diffused reflectance measurement was made. In the second measurement, the exit of the reflectance sphere was allowed to stay opened and let all the light got out. In the third measurement, the light has allowed going through the reflectance sphere and has got into the transmittance sphere and finally has collided the exit wall of the sphere. In this case the diffused transmittance value was measured. Again, in the third measurement, the collimated light accepted as returned on the same way it came without scattering. In the fourth measurement the light source of the system was closed and the light captured by the transmittance sphere dedector was measured when there were no tissues or light in. Theoretically there should be no lights that catched by the dedector but some minimal values have been recorded because of the noise in the environment (such as fluorescent light, the light coming out from LCD screens, etc). Every measurement repeated three times and the records of them have been saved. After the system optimized and become ready for the measurement of the tissues, the preparation of the tissue samples has been done [31].

2.2   The Inverse Adding Doubling Method

The purpose of the IAD method is to give fast and accurate solutions for scattering problems. The main working system of the IAD method is to find a solution to radiative transport equation which we mentioned earlier, for opposite surfaces [32]

The most important advantage of the IAD method is that it can give repetitive solutions with computer assitance, furthermore meanwhile giving enough flexibility to take into account anisotropy factors and internal reflections from the samples [26].

The method consists of four stages:

1. The choice of optical parameters to be measured

2. Counting reflections and transmissions

3. Comparison of calculated and measured reflectance and transmittance

4. Repetition of the procedure until the estimated and measured values coincide with the desired accuracy

With the reasonable computer assistance the method gives chance for any intended accuracy to be achieved for all the measurements [26].

The methods consider a 3% of error or less as acceptable.

There is term 'doubling' in the method means that the ingoing and outgoing light angels of reflection and transmission can be used to calculate both transmittance and reflectance for a layer by superimposing one on the other and then gives the contributions to the total reflectance and transmittance [33].

Reflection and transmission in a certain layers that have two different thicknesses are calculated in order, first for the thin layer (single scattering) and then by doubling the thickness for any layer [34].

The doubling procedure can be extended to heterogeneous layers in the purpose of modeling multilayer tissues or also calculating the internal reflections caused by refractive index, and this whole procedure gives the term of 'doubling' to the method.

The adding-doubling method is a numerical technique for to solve the one-dimensional transport equation. Other methods, such as Monte Carlo method, were not a good solution in regards to that [35].

It also can be used for Medias with two conditions: One is an arbitrary phase and second is an arbitrary angular distribution of the spatially uniform incident radiation.

This is why the losses for the size and side of the light cannot be calculated for the finite beam.

$$I_{ref}(\eta_c) = \int_0^1 I_{in}(\eta_c')R(\eta_c', \eta_c)2\eta_c'\,d\eta_c',$$ [Eqn. 4]

Where $I_{in}(\eta_c)$, is arbitrary incident radiance angular distribution, η_c is the cosine of the polar angle and $R(\eta_c', \eta_c)$ is the reflection redistribution function determined by the optical properties of the slab.

With obvious substitution of the transmission redistribution function $T(\eta_c', \eta_c)$, the distribution of the transmitted radiance can be expressed [36].

If M quadrature points are selected to span over the interval (0, 1), the respective matrices can approximate the reflection and transmission redistribution functions:

$$R\left(\eta_{ci}', \eta_{cj}\right) \rightarrow R_{ij}; \quad T\left(\eta_{ci}', \eta_{cj}\right) \rightarrow T_{ij}.$$ [Eqn. 5]

These matrices regarding as the reflection and transmission operators were in order. If a slab with boundaries indexed as 0 and 2 is comprised of two layers, (01) and (02), with an internal interface 1 between the layers, the reflection and transmission operators for the whole slab (02) can be expressed as:

$$T^{02} = T^{12}(E - R^{10}R^{12})^{-1}T^{01},$$

$$R^{20} = T^{12}(E - R^{10}R^{12})^{-1}R^{10}T^{21} + R^{21},$$

$$T^{20} = T^{10}(E - R^{12}R^{10})^{-1}T^{21},$$ [Eqn. 6]

$$R^{02} = T^{10}(E - R^{12}R^{10})^{-1}R^{12}T^{01} + R^{01},$$

Where E is the identity matrix defines in this case as

$$E_{ij} = \frac{1}{2\eta_{ci}w_i}\delta_{ij},$$ [Eqn. 7]

where

wi is the weight assigned to the ith quadrature point

δij is a Kroneker delta symbol, $\delta_{ij} = 1$ if i = j, and $\delta_{ij} = 0$ if i ≠ j

By taking advantage of these equations and making use of the methods described above the one can obtain both absorption and scattering coefficients from the measured diffuse reflectance Rd and diffuse transmittance Td.

To have the results from IAD method one must enter the anisotropy factor *g* and the refractive index *n* as input parameter to the programme.

The IAD method has been successfully applied to determine optical parameters of blood, human and animal dermis, brain tissues, mucous tissues, cranial bone and other soft tissues in the wide range of wavelengths.

2.3 Preparation of Tissue Samples

The tissue samples that have been used for actual assestments were obtained from Bezmialem Hospital and used for this study were pancreas normal (healthy), pancreas tumor tissues. Beforehand non-cancerous tissues different from pancreas have been examined as a preliminary study.

Tissues were collected intra operatively and then delivered to the Medical Lasers Laboratory at Boğaziçi University Institute of Biomedical Engineering immediately to have the measurements. The reason why the measurements were done in such a short notice is that they were needed be measured when they were still fresh. Human tissues will survive after biopsy for 24 hours at average [37-42].

A specific diameter was needed for the DIS system. As a precaution a plastic circular plaster was put in between the slides in order to prevent the leakage of tissues and then the tissue was prepared according to fit in this particular plaster afterwards the other slide closed on the other (Figure 2.10).
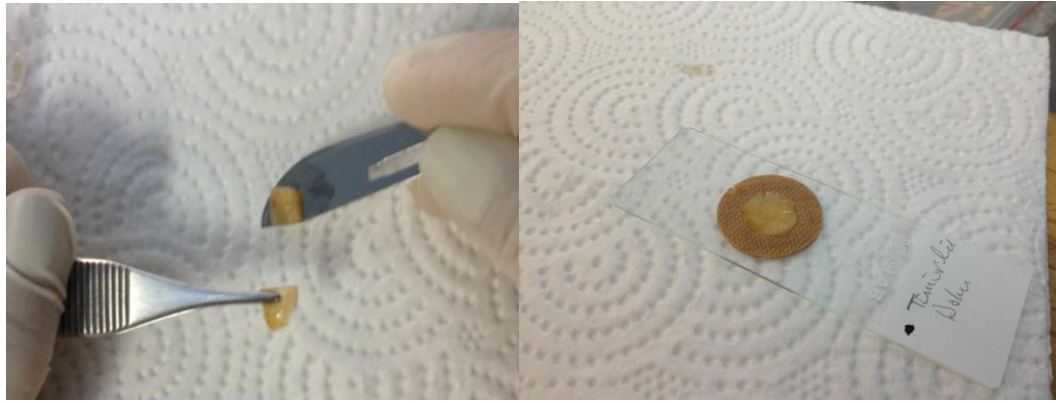
Figure 2.10 Preparation of a tissue sample for putting in the plaster

2.4   The Measurement Of The Optical Properties Of Healthy and Cancerous Tissues

In Prahl's IAD, some paremeters are needed to run the programme and one of them is the thickness of the sampes. But this thickness should not be the thickness of the tissue only. Because we put the entire slide into the sample part of the DIS system, the thickness of the entire slide is needed. So before or after the measurements, this thickness must be calculated with a micrometer.

Figure 2.11 Micrometer
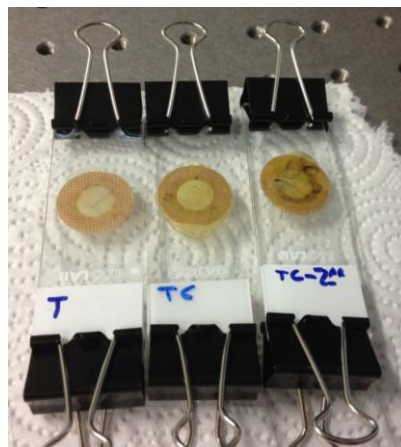
Figure 2.12 Prepared tissues in the slides

At this point of the study, the only parameter left needed to run the IAD programme was the MR and MT.

The prepared slides put in between the Reflection Sphere (RS) and Transmittance Sphere (TS)

Tissue slides in the DIS system during a measurement
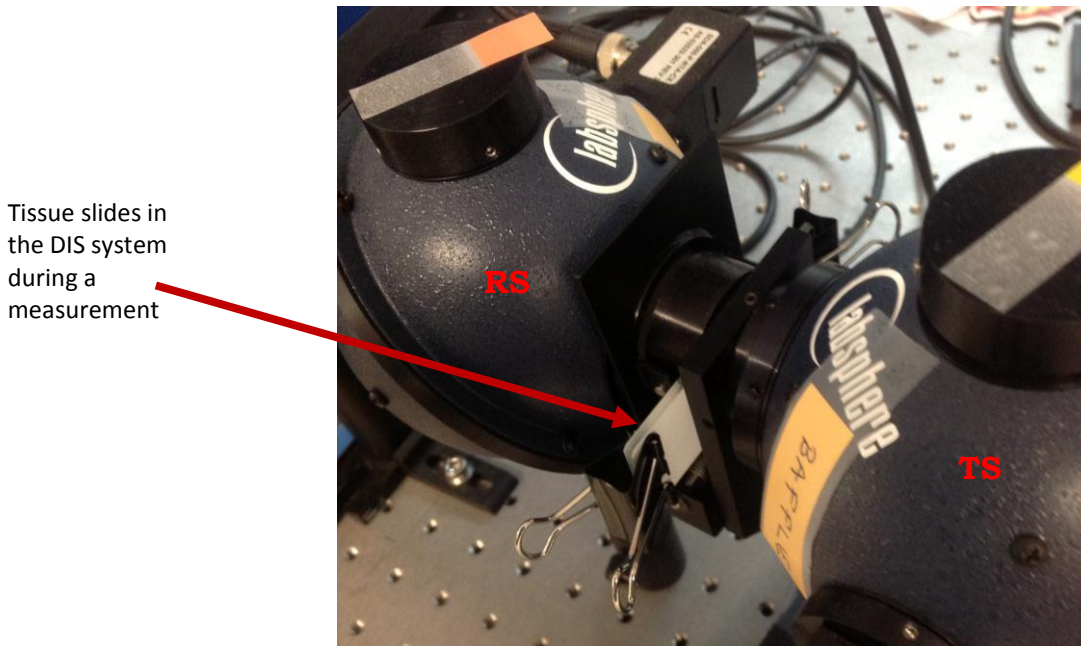
Figure 2.13 Tissue slides in the DIS system during measurements

RS: Reflection Sphere, TS: Transmittance Sphere

During this measurement, two steps were taken. First, to calculate the MR, the system connected with the lock-in Amplifier only from the first (reflectance) sphere via Reflectance Wire. Before setting up the system, it is better to check if the light interacts with the tissue in an appropriate way. To do that, system sets to 600nm inputs to give red light. And from the back of the transmittance sphere, this red light can be checked and seen if it was on the tissue in an appropriate way to have the measurement or not. After this process's complete, the system can be set up to 400nm and 700 nm (In all measurements the scan step value was 5nm) despite that the fact the only meaningful results could be taken between the ranges of 500nm and 650nm. The reason why 500nm and 650nm range have been chosen more important than the other wavelengths in the visible spectrum was because of the light source in our whole system was not sufficient enough. The light intensity that was taken from the halogen lamp in the system was at the same level of the environment noise with other wavelengths. And that was why we choosed 500nm and 650nm range in the study. After the system is set, the process can

be started. When the light comes into the first sphere and collides with the tissue, some reflection beams scatter because of the interaction between the light and the tissue and the Reflectance Dedector catches these reflections and afterwards transform them into electrical signals and send them to the computer which is connected with the entire DIS system [43-46]. To have better results for measuring the reflection and scattering the inner surface of the both sphere was made of a special component, which was made it easier for the light to diffuse inside the spheres [47-51]. After the process for the reflectance was done the same process applied for Transmittance Sphere too. But this time, the Transmittance Dedector cathes the beams that transmitted through the tissue in the second sphere.
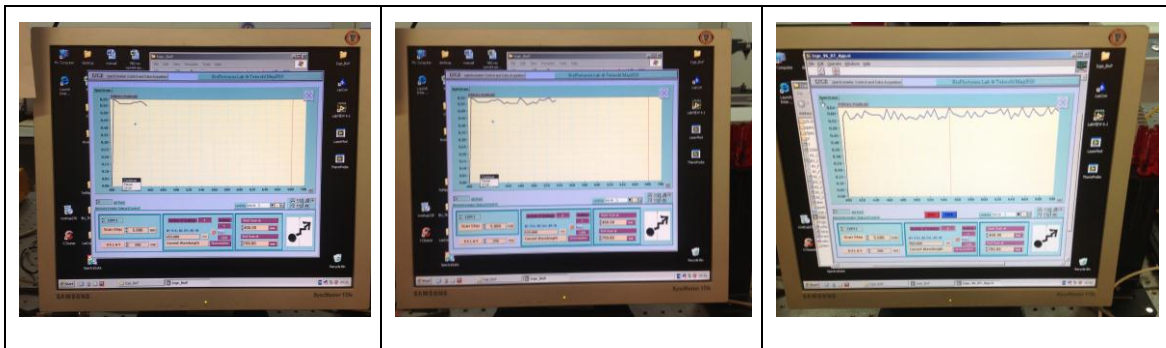
Figure 2.14 Pictures taken from three different stages of the measurement in sequence

Table 2.1 The stages of the computer program

Stages	Computer Processes
Stage 1	The incoming light beam gets into the DIS system
Stage 2	The light begins to diffuse in the spheres wavelength of 400 nm and 700 nm with 5nm increasements
Stage 3	The scattering and transmitting light sensed by the dedectors
Stage 4	The computer which is connected to the Double Integrating Sphere System begins to convert optical data to electronical signals
Stage 5	The computer program begins to show how the tissue and light interacts

Stage 6	The computer program gives a graphic for the values of transmittance and reflection coefficients with corresponding wavelengths

Same process has applied for every different tissue we obtained from the hospital for one time only.

CHAPTER 3

RESULTS AND DISCUSSIONS

3.1 Preliminary Study

In this part of the study some measurements have been made as a preliminary assay with non-cancerous tissues like lipid tissue, liver tissue, small intestine tissue and pancreas tissue.

Table 3.1 The Absorption Coefficients and Scattering Coefficients of Non-Cancerous Tissue Samples

Wavelength [nm]	LIVER μ_a	LIVER μ_s	LIPID μ_a	LIPID μ_s	S. INTESTINE μ_a	S. INTESTINE μ_s	PANCREAS μ_a	PANCREAS μ_s
500.00	200.00	0.10	0.07	4.17	1.84	2.10	0.00	23.84
505.00	200.00	0.10	6.65	0.00	0.84	10.80	1.45	2.08
510.00	1.11	9.13	0.28	2.40	2.46	2.00	0.42	11.05
515.00	13.75	0.00	7.27	0.00	19.86	0.00	0.29	9.22
520.00	13.75	0.00	7.27	0.00	19.86	0.00	9.05	0.00
525.00	3.98	1.69	1.52	0.00	5.65	0.00	0.68	4.47
530.00	1.49	3.93	0.00	0.00	2.84	2.73	1.17	3.20
535.00	13.04	0.00	0.00	0.00	3.06	1.74	3.57	0.00
540.00	4.26	1.61	1.30	0.00	2.64	1.96	0.64	4.36
545.00	5.16	2.13	1.39	0.00	2.12	2.85	0.62	5.20
550.00	8.29	0.00	0.12	0.00	1.17	5.55	1.96	1.10
555.00	2.55	4.95	0.06	0.00	1.62	4.65	0.74	4.18
560.00	1.63	3.48	0.00	0.00	5.24	0.43	1.29	2.30
565.00	1.89	4.66	0.06	0.00	3.16	1.47	10.36	0.00
570.00	2.49	4.37	0.16	0.00	1.87	3.09	0.62	4.59
575.00	1.44	7.44	0.15	0.87	4.24	0.00	0.48	6.11
580.00	1.54	11.12	0.05	0.85	1.63	3.78	1.13	2.55
585.00	2.55	1.99	0.36	0.00	1.57	3.07	1.79	1.61
590.00	5.97	0.00	0.71	0.00	1.50	2.70	0.59	3.91
595.00	1.12	3.33	0.00	0.16	2.38	1.80	0.75	3.99
600.00	1.05	6.44	0.00	0.59	1.55	2.83	3.00	0.00
605.00	2.44	5.68	0.42	0.68	1.10	3.66	1.63	1.07
610.00	15.84	0.00	7.42	0.00	3.95	0.59	0.31	8.70
615.00	15.84	0.00	7.42	0.00	0.79	4.52	0.28	6.55
620.00	15.84	0.00	7.42	0.00	0.42	7.13	0.47	5.22
625.00	2.05	3.73	0.50	0.58	0.42	8.27	0.92	3.01
630.00	1.00	12.77	0.06	1.57	0.92	2.39	1.75	1.67
635.00	0.48	11.90	0.01	2.37	16.89	0.00	1.28	1.43
640.00	11.88	0.00	6.09	0.00	16.89	0.00	0.20	12.87
645.00	2.69	1.97	0.68	0.00	0.63	4.81	0.00	29.36
650.00	14.17	0.00	7.15	0.00	1.32	3.47	0.16	10.13
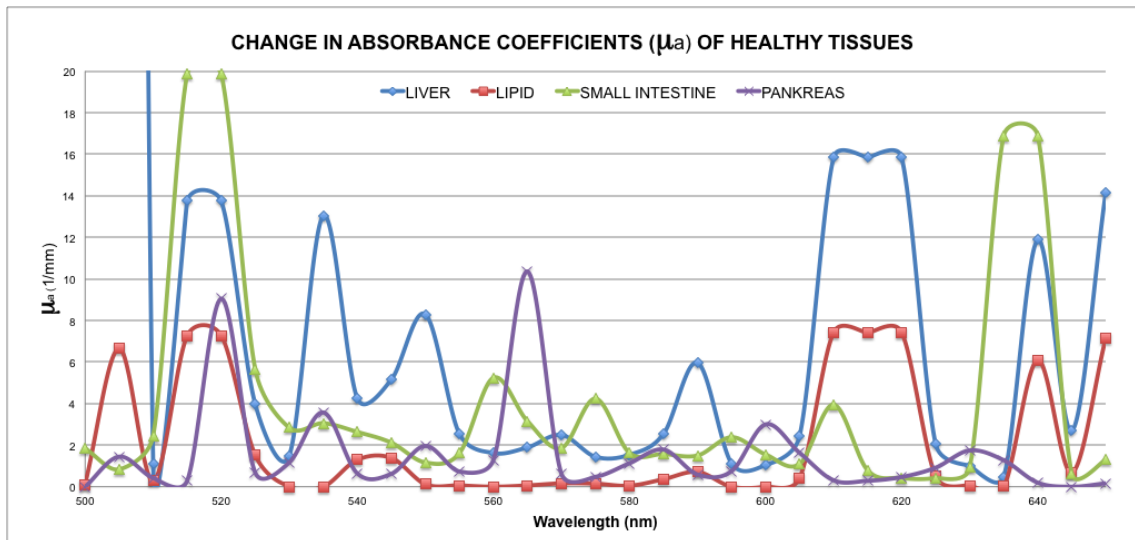
Figure 3.1: Change in Absorbance Coefficients of Healthy Tissues

At the very first look; it could be seen that the lowest absorption peaks would have been observed for lipid tissue.

At the most of its absorption trajectory the lipid tissue has been followed the baseline values. It has been showed peaks around at 510nm, 520nm, 545nm, 610nm, 640nm and 650nm. Between 545nm and 610nm the absorption trajector for lipid tissue has been followed the baseline, so it could be said that between 545nm and 610nm lipid tissue has not absorbed any wavelenght. The biggest value for the highest peak for the lipid tissue was 8 mm^{-1}. All of this could be a valuable data to know when trying to diagnos the healthy lipid tissue from the cancerous lipid tissue with making a comparison. But this data alone was not sufficient enough to have a general idea of how lipid tissue interacts with light.

And the second lowest absorption peaks have been observed for healthy pancreas tissue. It has been showed eight peakts at different wavelength which were 510nm, 520nm, 530nm, 550nm, 570nm, 590nm, 600nm and 630nm. Absorption coefficient trajectory of the healthy pancreas tissue have never been followed the baseline completely like healthy lipid tissue.

So, it could be said that healthy pancreas tissue has absorbed more light than the lipid tissue has did. The highest peak point for the healthy pancreas tissue was at 10 mm^{-1} which was bigger than the highest peak point of the lipid tissue. So, the healthy pancreas tissue has had more interaction with light than the lipid tissue had, in terms of absorption criteria. Knowing that at which wavelengths a tissue showed absorption

peaks, could be a valuable data for light based diagnosis of cancer by using comperative techniques, though this data alone was not sufficient and could be accepted as a general look and further investigation was needed.

The highest peak points have been observed for liver tissue and small intestine tissue. Both tissues have been showed the highest peak points at around 14 mm^{-1}, 16mm^{-1}, 17mm^{-1} and higher than 20mm^{-1}. Healthy liver tissue had more absorption than the small intestine tissue. So it could be interpreted as that the liver tissue had a very effective and active absorption structure when it interacted with light at visible spectrum. The highest peak point for both tissues which was more than 20 mm^{-1} has been obserbed at around 510 nm. 520 nm was the only wavelength where all of the four tissues had peak.

Why all of these tissues showed a peak at the same point could be a very valuable question which needed further investigation. The similar concept have been seen at around 610 nm and 640 nm but none of these two wavelengths have been showed the contingency which 520 nm wavelength have been showed. 520 nm point needed further investigation and could be a valuable data for light based diagnosis of the cancer.
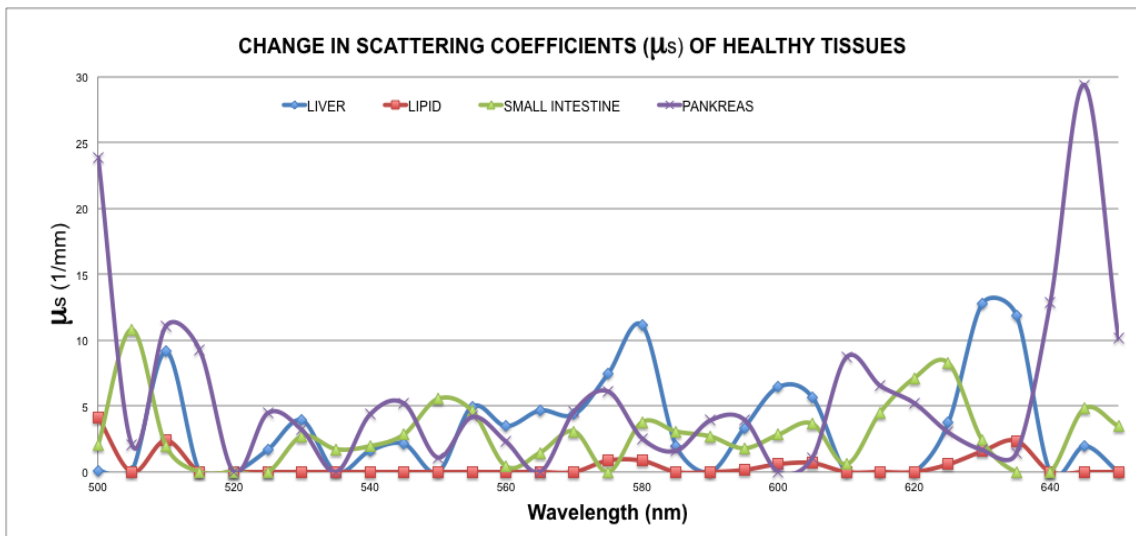
Figure 3.2: Change in Scattering Coefficients of Healthy Tissues

In general, it could be said that all four tissues have showed similar scattering trajectories. The highest scattering coefficient in the healthy tissues has been observed for healthy pancreas tissue at 25mm^{-1} and 30mm^{-1} points. The scattering coefficient trajectory of the lipid tissue had followed the baseline values almost for all along the graphic. So, it could be said that the lowest scattering structure was the lipid tissue.

Other tissues, which are liver, small intestine and pancreas, have showed very similar trajectories for scattering except the peaks, which were mentioned above for the pancreas tissue. This behavior of the health pancreas tissue could be a valuable data for light based diagnosis of the cancer.

The most interesting point for both the absorption coefficients and scattering coefficients have been observed at 520nm wavelength. At both graphics, at 520nm, all of four tissues showed peaks at high values. This data alone was the most important information, which could be gained by the preliminary study part of this study, although this has no statistical meaning.

3.2 Main Assays

In this part of the study main assays and measurement have been made and stated.

In next sections tables with absorption coefficients and scattering coefficients of **healthy pancreas tissues** have been showed with their average and standard deviation results for all 8 patients.

Table 3.2 Absorption Coefficients of Healthy Pancreas Tissues for 8 Patients with Corresponding Average Values and Standard Deviations

Wavelength [nm]	μ_{a1}	μ_{a2}	μ_{a3}	μ_{a4}	μ_{a5}	μ_{a6}	μ_{a7}	μ_{a8}	μ_{a_AVG}	μ_{a_STD}
500	0.98	0.00	10.51	200.00	1.59	1.62	0.41	2.78	27.24	65.37
505	1.11	0.00	5.92	0.60	1.17	1.51	1.50	2.23	1.75	1.69
510	1.41	0.04	3.78	0.56	1.23	0.85	1.50	1.92	1.41	1.05
515	0.93	0.25	3.77	0.39	1.35	1.20	14.77	1.72	3.05	4.55
520	10.80	0.37	3.52	1.06	1.16	0.30	1.00	1.98	2.52	3.27
525	1.89	0.44	2.70	1.06	0.81	0.00	0.93	1.61	1.18	0.80
530	0.86	0.52	2.39	0.75	1.80	0.00	2.20	1.29	1.23	0.79
535	2.55	0.66	1.87	0.89	1.18	0.00	2.18	1.74	1.38	0.80
540	0.64	0.51	1.56	1.29	1.55	3.18	2.11	1.90	1.59	0.80
545	2.88	0.54	1.34	1.68	1.23	3.63	1.57	2.22	1.89	0.92
550	0.72	0.45	1.22	2.05	1.64	0.00	1.07	1.44	1.07	0.62
555	1.11	0.61	1.17	1.09	1.83	0.00	1.47	1.34	1.08	0.52
560	2.49	0.55	1.02	1.11	1.61	4.63	2.60	1.04	1.88	1.24
565	1.07	0.57	1.01	1.22	1.49	0.00	2.19	0.94	1.06	0.60
570	1.01	0.54	1.01	1.21	1.81	3.91	2.66	1.13	1.66	1.04
575	1.31	0.57	1.05	1.35	1.73	4.09	1.50	1.24	1.60	0.99
580	0.95	0.58	1.00	1.59	1.16	2.95	1.45	1.30	1.37	0.67
585	0.65	0.51	1.14	1.68	1.44	3.11	0.92	1.29	1.34	0.76
590	3.20	0.58	1.22	1.12	1.46	3.63	1.47	1.70	1.80	0.99
595	0.70	0.49	1.29	0.88	1.49	4.89	1.95	1.35	1.63	1.31
600	0.56	0.38	1.34	1.21	0.66	3.77	1.23	1.50	1.33	1.00
605	0.70	0.45	1.57	2.55	0.86	0.00	1.91	1.64	1.21	0.79
610	0.28	0.30	1.67	1.28	1.05	4.11	4.02	2.08	1.85	1.40
615	8.70	0.09	1.58	1.40	1.12	2.18	3.69	1.60	2.54	2.51
620	0.86	0.08	1.93	0.52	1.12	2.62	0.54	1.48	1.14	0.78
625	9.85	0.09	2.99	0.71	1.16	3.34	0.89	2.40	2.68	2.92
630	0.90	0.06	1.77	0.49	1.19	0.00	0.66	1.59	0.83	0.62
635	0.68	0.00	1.74	9.34	1.21	0.00	1.50	1.27	1.97	2.85
640	0.26	0.00	1.46	9.34	1.27	0.03	0.78	2.26	1.92	2.90
645	0.81	0.00	1.33	0.51	12.24	3.03	15.00	1.81	4.34	5.47
650	0.57	0.00	1.26	8.83	1.18	0.50	2.42	1.94	2.09	2.65

Table 3.3 Scattering Coefficients of Healthy Pancreas Tissues for 8 Patients with Corresponding Average Values and Standard Deviations

Wavelength [nm]	μ_{s1}	μ_{s2}	μ_{s3}	μ_{s4}	μ_{s5}	μ_{s6}	μ_{s7}	μ_{s8}	μ_{s_AVG}	μ_{s_STD}
500	5.63	2.44	0.00	0.10	0.00	0.00	10.42	1.88	2.56	3.49
505	2.87	5.37	2.05	13.41	0.36	0.52	2.28	2.23	3.64	3.97
510	3.19	9.74	3.35	5.87	0.24	0.00	3.17	2.46	3.50	2.93
515	5.89	7.78	2.75	16.28	0.01	0.00	0.00	2.49	4.40	5.23
520	0.00	7.72	2.51	10.70	0.01	0.00	6.86	1.79	3.70	3.89
525	1.65	6.32	2.62	7.56	0.00	0.00	6.29	1.83	3.28	2.82
530	4.27	5.43	2.26	7.06	0.00	0.00	2.92	1.83	2.97	2.34
535	0.96	3.97	2.30	7.84	0.00	0.00	2.61	0.89	2.32	2.45
540	5.31	4.93	2.30	5.98	0.00	0.00	2.50	0.53	2.69	2.29
545	0.38	4.70	2.16	3.32	0.00	0.00	3.94	0.02	1.81	1.84
550	4.68	5.53	2.10	3.64	0.00	0.00	5.08	0.74	2.72	2.16
555	2.75	4.91	2.00	7.37	0.00	0.00	4.46	0.77	2.78	2.46
560	0.72	4.55	2.08	4.98	0.00	0.00	2.10	1.04	1.93	1.80
565	2.82	5.03	2.00	6.23	0.00	0.00	2.01	1.15	2.41	2.10
570	3.23	4.97	1.99	6.51	0.00	0.00	1.75	0.87	2.41	2.20
575	2.15	5.36	1.99	4.38	0.00	0.00	3.18	0.77	2.23	1.85
580	3.13	5.70	2.19	2.53	0.00	0.00	2.71	0.79	2.13	1.77
585	4.04	5.41	2.14	2.17	0.00	0.00	5.18	0.92	2.48	2.04
590	0.00	4.63	2.19	6.43	0.00	0.00	2.71	0.60	2.07	2.27
595	4.07	5.13	2.27	6.12	0.00	0.00	2.44	1.20	2.65	2.14
600	4.21	8.21	2.34	3.72	0.00	0.00	3.58	1.20	2.91	2.52
605	3.26	6.94	2.31	1.95	0.01	0.00	1.62	1.27	2.17	2.08
610	7.15	6.91	2.51	2.44	0.01	0.00	0.00	0.86	2.48	2.79
615	0.00	9.48	2.60	3.87	0.00	0.00	0.00	1.52	2.18	3.08
620	3.10	8.68	2.04	5.42	0.00	0.00	5.40	1.60	3.28	2.83
625	0.00	8.48	0.94	4.32	0.01	0.00	4.47	0.61	2.35	2.90
630	2.82	9.65	2.43	8.65	0.01	0.00	6.79	1.44	3.97	3.60
635	2.54	7.41	2.29	0.00	0.00	0.00	2.81	1.98	2.13	2.30
640	6.84	7.65	2.89	0.00	0.00	0.00	13.28	0.84	3.94	4.57
645	2.21	3.44	3.14	5.85	0.00	0.00	0.00	1.31	1.99	1.96
650	6.50	1.62	3.20	0.00	0.01	0.00	0.92	1.19	1.68	2.08

In next sections tables with absorption coefficients and scattering coefficients of **cancerous pancreas tissues** have been showed with their average and standard deviation results for all 8 patients.

Table 3.4 Absorption Coefficients of Cancerous Pancreas Tissues for 8 Patients with Corresponding Average Results and Standard Deviations

Wavelength [nm]	μ_{a1}	μ_{a2}	μ_{a3}	μ_{a4}	μ_{a5}	μ_{a6}	μ_{a7}	μ_{a8}	μ_{a_AVG}	μ_{a_STD}
500	0.69	0.00	1.57	0.13	2.31	3.10	0.08	1.77	1.21	1.08
505	0.62	0.00	1.00	7.93	3.39	1.17	0.29	1.55	1.99	2.44
510	0.77	0.01	1.26	0.46	1.74	0.00	0.35	1.64	0.78	0.65
515	0.57	0.12	1.17	0.57	2.16	0.00	0.22	1.66	0.81	0.73
520	0.96	0.16	1.21	0.60	1.82	4.77	0.24	1.40	1.39	1.38
525	0.79	0.19	0.91	0.75	1.43	4.21	0.23	1.08	1.20	1.20
530	1.14	0.23	0.96	0.62	1.38	0.00	0.26	0.76	0.67	0.45
535	2.04	0.29	0.77	1.44	1.12	0.00	0.34	0.61	0.83	0.63
540	1.82	0.22	0.70	0.86	0.97	0.00	0.27	0.62	0.68	0.53
545	0.78	0.25	0.71	2.44	0.94	3.93	0.36	1.24	1.33	1.17
550	0.52	0.21	0.66	1.15	0.87	0.00	0.20	1.29	0.61	0.44
555	0.80	0.27	0.62	0.77	1.08	0.00	0.17	0.51	0.53	0.34
560	0.96	0.28	0.59	0.55	0.84	0.00	0.41	1.44	0.63	0.42
565	1.41	0.26	0.58	1.23	0.90	0.00	0.35	1.69	0.80	0.56
570	0.77	0.24	0.62	0.67	0.94	5.20	0.18	1.35	1.24	1.53
575	0.81	0.25	0.59	0.63	1.04	4.84	0.19	1.28	1.20	1.42
580	2.48	0.24	0.61	1.39	1.15	5.19	0.15	0.87	1.51	1.55
585	0.82	0.25	0.64	0.89	1.20	5.23	0.13	1.08	1.28	1.53
590	1.06	0.27	0.66	1.55	1.19	1.76	0.26	1.38	1.02	0.53
595	1.04	0.23	0.63	0.80	1.08	5.12	0.44	1.03	1.30	1.47
600	1.10	0.17	0.74	0.30	1.09	0.00	0.14	0.72	0.53	0.41
605	1.44	0.20	0.79	0.72	1.23	4.36	0.24	0.95	1.24	1.25
610	2.07	0.13	0.72	7.63	1.26	4.96	0.22	1.10	2.26	2.49
615	0.41	0.04	0.71	0.50	1.54	0.00	0.10	1.12	0.55	0.51
620	0.40	0.04	0.96	0.57	1.69	5.12	0.07	1.13	1.25	1.55
625	0.52	0.05	2.24	0.64	2.37	4.25	0.08	1.22	1.42	1.36
630	0.34	0.02	0.93	0.44	1.19	0.00	0.07	1.16	0.52	0.47
635	1.02	0.00	0.52	0.17	0.90	3.55	0.14	1.12	0.93	1.07
640	3.02	0.00	0.51	0.11	0.90	4.04	0.02	1.18	1.22	1.41
645	2.88	0.00	0.53	0.33	0.99	21.74	0.17	1.20	3.48	6.95
650	0.02	0.00	0.68	0.03	1.03	0.86	0.06	11.62	1.79	3.74

Table 3.5 Scattering Coefficients of Cancerous Pancreas Tissues for 8 Patients with Corresponding Average Results and Standard Deviations

Wavelength [nm]	μ_{s1}	μ_{s2}	μ_{s3}	μ_{s4}	μ_{s5}	μ_{s6}	μ_{s7}	μ_{s8}	μ_{s_AVG}	μ_{s_STD}
500	16.16	1.03	2.17	18.37	1.46	0.00	9.03	0.00	6.03	7.05
505	9.71	2.00	2.99	0.00	0.00	0.00	7.24	0.01	2.74	3.53
510	4.28	4.09	2.13	11.86	1.59	0.00	3.28	0.00	3.41	3.55
515	6.10	3.61	2.11	4.43	1.01	0.00	7.54	0.00	3.10	2.63
520	3.62	3.28	1.81	3.78	1.16	0.00	5.25	0.00	2.36	1.79
525	4.30	2.81	2.12	2.63	1.22	0.00	6.49	0.01	2.45	2.05
530	2.84	2.41	1.73	3.43	0.97	0.00	5.38	0.00	2.09	1.71
535	1.18	1.76	1.82	1.34	1.03	0.00	4.20	0.00	1.42	1.24
540	1.64	2.19	1.80	2.11	1.01	0.00	4.65	0.00	1.67	1.39
545	3.89	2.18	1.64	0.00	0.88	0.00	4.30	0.00	1.61	1.62
550	5.49	2.36	1.61	1.54	0.93	0.00	5.59	0.00	2.19	2.07
555	3.74	2.00	1.62	2.86	0.60	0.00	5.58	0.00	2.05	1.83
560	2.87	1.91	1.60	2.67	0.82	0.00	2.84	0.00	1.59	1.12
565	1.97	2.12	1.54	1.46	0.74	0.00	3.88	0.00	1.46	1.19
570	3.20	2.20	1.46	2.90	0.69	0.00	6.10	0.00	2.07	1.91
575	2.93	2.38	1.50	2.51	0.60	0.00	4.30	0.00	1.78	1.43
580	0.67	2.42	1.47	1.23	0.54	0.00	5.00	0.00	1.42	1.55
585	3.06	2.40	1.50	1.94	0.59	0.00	5.39	0.00	1.86	1.69
590	2.30	2.15	1.50	0.81	0.71	0.00	3.60	0.00	1.38	1.17
595	2.60	2.16	1.60	1.93	1.00	0.00	1.97	0.00	1.41	0.92
600	2.30	3.64	1.51	4.12	1.18	0.00	5.20	0.00	2.24	1.80
605	1.15	3.07	1.58	1.99	1.22	0.00	3.84	0.01	1.61	1.26
610	0.66	3.43	1.86	0.00	1.24	0.00	3.43	0.00	1.33	1.36
615	4.84	4.38	1.90	3.36	0.96	0.00	5.31	0.00	2.59	2.03
620	6.27	4.02	1.34	2.98	0.83	0.00	4.87	0.01	2.54	2.20
625	5.70	3.71	0.01	2.23	0.17	0.03	4.76	0.00	2.08	2.22
630	8.02	4.29	1.49	2.53	1.38	0.00	4.76	0.01	2.81	2.57
635	2.79	3.65	2.51	7.13	1.91	0.00	3.30	0.08	2.67	2.11
640	0.00	3.32	2.74	8.41	2.00	0.00	12.17	0.00	3.58	4.17
645	0.00	1.47	2.59	2.72	1.83	0.00	4.40	0.00	1.63	1.49
650	14.82	0.86	1.76	11.49	1.90	0.00	3.87	0.00	4.34	5.29

3.3 Comparison Of Main Assays

In this part of the study a comparison between the healthy and cancerous pancreas tissues for both absorption coefficients and scattering coefficients have been made to see how they have interacted with the same wavelength. This examination could be accepted as a key point in this study to gain a better understanding of how pancreas behave at different wavelength when it was healthy stage and cancerous stage.
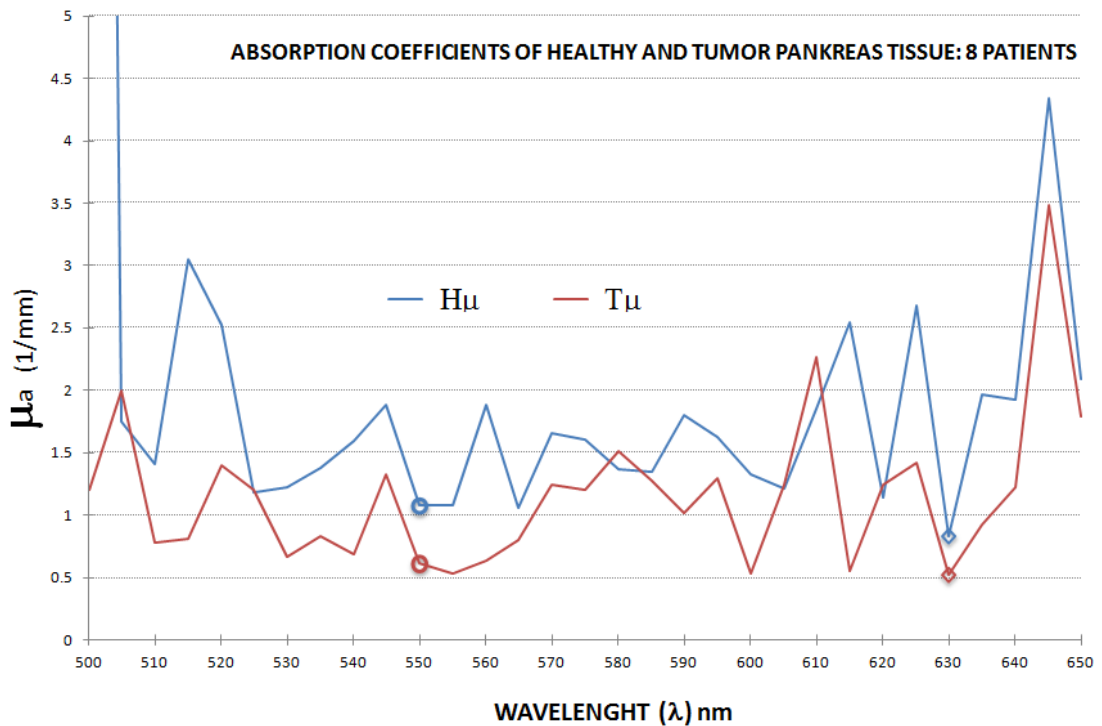
Figure 3.3: Comparison of Absoprtion Coefficients of Healthy and Tumor (Cancerous) Pancreas Tissues for 8 Patients

The absorption coefficients of healthy and cancerous pancreas tissues for eight patients have been showed on the graphic above. It could be seen that both the healthy and cancerous pancreas tissues have absorbed light between 500nm and 650nm and none of the absorption trajectories for healthy or cancerous pancreas tissues have never decreased to the bottom line. So, both healthy and cancerous *pancreas* tissues have absorbed the wavelengths between 500nm and 650nm spectrum. If a comparison has been made between all eight healthy and cancerous pancreas tissue samples it could be seen that healthy pancreas tissues had higher peak points than cancerous pancreas tissues almost at every wavelength. The highest peak point for cancerous pancreas tissue have been observed at 3.5mm^{-1} but on the other hand the highest peak point for healthy cancerous tissue have been observed at points bigger than 5mm^{-1}. This could be interpreted as that the healthy pancreas tissue had absorber structure than the cancerous tissue. So, it could be said that the cancer had changed the healthy tissue's structure and its optical properties therefore its interactions with light had been altered. This data had been obtained from all eight patients and therefore could be accepted as a proof that supports our hypothesis. The statistical significant differences have been indicated as

circles and squares on the graphic above, but the statistical investigations will be given in the chapter 3.4.
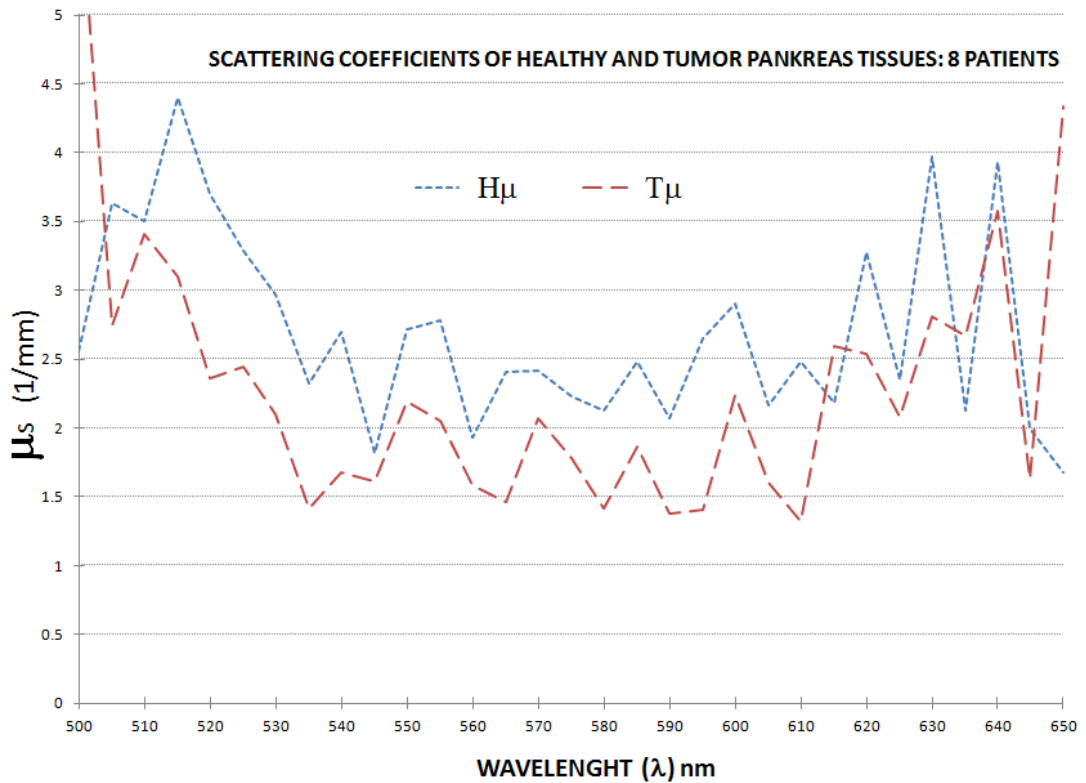

Figure 3.4: Comparison of Scattering Coefficients of Healthy and Tumor (Cancerous) Pancreas Tissues for 8 Patients

The scattering coefficients of healthy and cancerous pancreas tissues for eight patients have been showed on the graphic above. In general the same concept which has been accepted for absorption coefficients could be accepted for the scattering coefficients too which was that healthy pancreas tissues had higher absorption values than the cancerous pancreas tissues. In general the highest peak point values have been observed for cancerous tissues which was the exact opposite case for absorption coefficients. The highest peak point of the scattering coefficients of the cancerous tissues was gone beyond 5mm^{-1}. But the highest peak point of the scattering coefficients of the healthy tissues have been observed at 4.5mm^{-1}. And again, in general, the trajectories of both healthy pancreas tissues and cancerous pancreas tissues have showed similarities. None of the eight patients have been showed a bottomline value for both healthy and cancerous tissue which could be interpreted as both healthy pancreas tissue and cancerous pancreas tissue have been scattered in the choosen wavelength range. All of the observations which have been taken from the graphic above could be interpreted as

that the healthy pancreas tissue had a more scattering structure than the cancerous healthy tissue. So, it could said that the cancer had changed the healthy tissue's structure and its optical properties therefore its interactions with light had been altered. This data had been obtained from all eight patients and therefore could be accepted as a proof which supports our hypothesis.

3.4 Statistical Analysis

In the purpose of getting meaningful results from the study, *T-Test* has been applied as a statistical analysis for absorption coefficients and scattering coefficients. By using the T-Test we have observed if there was any significant differences between the tissue samples. T-Test has been applied to both absorption coefficients and scattering coefficients for healthy and cancerous pancreas tissue samples.

According to the result of two tailed and paired T-Test; the only significant differences were recorded at 550nm and 630nm wavelength. It could be interpreted as that, at 550nm and 630 nm wavelengths, healthy and cancerous pancreas tissues have showed significantly different absorption coeficients because of the pancreas tissue's structure and optical properties. With this significant difference it was possible to be said that at these wavelengths both tissues could be seperated by using the DIS system. This data will help pathology and histology to confirm the assessment.

On the other hand; there were no statistical difference has been found for the scattering coefficients at any wavelenght.

3.5 Pathological Results

In this part of the study, the pathological findings have been examined.

<u>For patient 1:</u>

Age: 55

Sex: Male

Type of the tumor: Malign pancreas neoplasm

Size: 1,2cmX1cmX0,5cm

Histological type: Ductal adenocarcinoma

Histological grade: II

For Patient 2:

Age: 69

Sex: Male

Type of the tumor: Malign pancreas neoplasm

Size: 4cmX3cmX3cm

Histological type: Ductal adenocarcinoma

Histological grade: III

For Patient 3:

Age: 48

Sex: Male

Type of the tumor: Malign pancreas neoplasm

Size: 4cmX2,5cmX2cm

Histological type: Primary or secondary type

Histological grade: Borderline

For Patient 4:

Age: 61

Sex: Male

Type of the tumor: Malign pancreas neoplasm

Size: 2,7cmx2 cmx2,5cm

Histological type: Ductal adenocarcinoma

Histological grade: III

For Patient 5:

Age: 83

Sex: Male

Type of the tumor: No sign of neoplasm at the pancreas

Size: 2,7cmX3cmX2cm

Histological type: Ductal adenocarcinoma

Histological grade: III

For Patient 6:

Age: 67

Sex: Female

Type of the tumor: Malign Pancreas Neoplasm

Size: 2,5cmX2cmX1,5cm

Histological type: Ductal adenocarcinoma

Histological grade: II

For Patient 7:

Age: 72

Sex: Male

Type of the tumor: Malign Pancreas Neoplasm

Size: 2,3cmX2cmX1,5cm

Histological type: Ductal adenocarcinoma

Histological grade: II

For Patient 8:

Age: 58

Sex: Female

Type of the tumor: Malign Pancreas Neoplasm

Size: 3,1cmX5cmX0,5cm

Histological type: Ductal adenocarcinoma

Histological grade: III

CHAPTER 4

CONCLUSIONS AND RECOMMENDATIONS

It was possible to be said that the hypothesis of the entire study has been proved. In the Chapter 3, it could be seen obviously that the optical charecteristics of cancerous and normal tissues were different for every single tissue sample. By that it could be possible to be said that the optical charecteristics of a healthy tissue have been changed with a neoplasm (cancer/tumor) growing inside of it and therefore its complete structure have been changed and so its interactions with light at every wavelength have been eventually changed. By examining the differences between the cancerous and healthy pancreas tissues, how a pancreas tissue, whether it was cancerous or non-cancerous, behaves between the range of 500nm and 650nm have been observed. The DIS system has been proved useful to distinguish these different behaviors of cancerous and non-cancerous tissues at any selected wavelength. With 5nm increasment steps, how a single tissue's cancerous and non-cancerous structure behaves at a specific wavelength between 500nm and 650nm have been observed and then have been compared among all 8 patients. To achieve a better understanding of these differencies T-Test has been applied as a statistical analyzes. And as a result of the statistical analyzes the only significant differencies have been observed at 550nm and 630nm. These results then have been compared with pathological results which were taken from the hospital. Histological type of all cancerous pancreas tissue samples were Ductal Adenocarcinoma. Their histological grades were between Grade II and Grade III. None of the cancerous pancreas tissue samples were Grade I or Grade IV. The type for the most of the cancerous pancreas tissue samples were Malign Neoplasm. The lowest age has been observed was 48. And the sizes of the cancerous pancreas tissue samples were various from 1,2cmX1cmX0,5cm (the smallest) to 4cmX2,5cmX2cm(the biggest). Therefore, as a result of a comparison with pathological findings, it was not possible to

be said that any of these finding such as grade level, age etc were related with outcome we have gained from the DIS system. Grade I and Grade IV levels, any age younger than 48, any other type rather than Ductal Adenocarcinoma have not been observed, but alone these findings alone were not enough to conclude the pathlogical results with the light interactions results. Therefore further investigations have been needed with more tissue samples. All of these findings could be a very sourceful and useful data for light based treatments and diagnosis of the pancreas cancer. To know exactly how cancerous pancreas tissue and non-cancerous pancreas tissue behaves at 550nm and 630nm could be used by researchers who deals with therapies like PhotoDynamic Therapy (PDT) or LLLT (Low Level Laser Therapy). Results of this study will be shed light on inspection of pathological changes of tissues, and improvement of clinical applications such as these therapies. Today, in almost every cancer surgeons still have troubles about locating the cancer and taking enough tissue from the patient who has cancer. By using light and tissue interaction methods like DIS and IAD, in future, there even might be no need left for pathological rooms in Operating Rooms. And in future, cancer surgeons might be able to use these kinds of systems for two purposes. One; is to locate the cancer (diagnosis). And the second one is, by making further investigations about the subject, diagnosing the cancer. So, this way, the doctors will not even need pathological assestments for cancer. This will both save time and unnecessary insicions or surgical techniques in ORs. But further investigations have been needed to understand other types of cancers and how they behave for specific wavelength. The entire study also could be expanded to Infrared region to find out other valuable datas for diagnosis and treatment aspects of cancer.

NOVELTY OF THE THESIS

The novelty of the thesis was to measure optical properties of different types of tissues in the same study but mainly focus on the pancreas cancer. The light and tissue interaction for more than just one type of tissue were observed in the study. *The novelty of the study was to compare healthy and cancerous pancreas tissues by taking into account the pathological results in every aspect such as size, grade etc*. The further study could be done in both ultraviolet and infrared regions which were two borders of the visible field. And in a further reasearch the number of the tissue samples could be increased too have more statistical meanings. But yet, all of this study was enough to prove that it was possible to understand how light interacted with cancerous and healthy pancreas tissue especially at 550nm and 630nm.

REFERENCES

[1]   Dhiraj K. Sardar & Brian G. Yust & Frederick J. Barrera & Lawrence C. Mimun & Andrew T. C. Tsin "Optical absorption and scattering of bovine cornea, lens and retina in the visible region" Lasers Med Sci (2009) 24:839–847

[2]   Anne GILLE-GENEST "Introduction to the Monte Carlo Methods" March 1, 2012

[3]   Ingemar Fredriksson, Marcus Larsson, Tomas Strömberg "Inverse Monte Carlo method in a multilayered tissue model for diffuse reflectance spectroscopy." 04/2012; 17(4):047004.

[4]   Hua-Jiang Wei, Da Xing, Jian-Jun Lu, Huai-Min Gu, Guo-Yong Wu, Ying Jin " Determination of optical properties of normal and adenomatous human colon tissues in vitro using integrating sphere techniques" 2005;11(16):2413-2419

[5]   Ashley J. Welch,Martin J.C. van Gemert, Willem M.Star "Definitions and Overview of Tissue Optics" 31 Aug 1995

[6]   Flock, S.T. ; Hamilton Cancer Centre ; Patterson, M.S. ; Wilson, B.C. ; Wyman, D.R. "Monte Carlo modeling of light propagation in highly scattering tissues. I. Model predictions and comparison with diffusion theory" Biomedical Engineering Journal Volume:36 Issue:12

[7]   Christoph Holmer, Kai S. Lehmann, Jana Wanken, Christoph Reissfelder, Andre Roggan, Gerhard Mueller, Heinz J. Buhr, Joerg-Peter Ritz "Optical properties of adenocarcinoma and squamous cell carcinoma of the gastroesophageal junction" Journal of Biomedical Optics 12   1 , 014025 January/February 2007

[8]   E Solomon, J Borrow, AD Goddard "Chromosome aberrations and cancer"
        Science 22 November 1991:Vol. 254 no. 5035 pp. 1153-1160

[9]   Berton Zbar, Gladys Glenn, Irina Lubensky, Peter Choyke, McClellan M.
        Walther, Gosta Magnusson, Ulf S.R. Bergerheim, Silas Pettersson, Mahul
        Amin, Kathy Hurley, W. Marston. Linehan "Original Articles: Kidney Cancer:
        Hereditary Papillary Renal Cell Carcinoma: Clinical Studies in 10 Families"
        The Journal of Urology Volume 153, Issue 3, Supplement , Pages 907-912,
        March 1995

[10]   http://en.wikipedia.org/wiki/Cancer - 01.07.2013

[11]   Giakos, G.C. ; Dept. of Electr. & Comput., Univ. of Akron, Akron, OH, USA ;
        Marotta, S. ; Narayan, C. ; Petermann, J. "Near infrared light interaction with
        lung cancer cells" Instrumentation and Measurement Technology Conference,
        1 - 6, 1091-5281

[12]   J. Baniel, R.S. Foster, R.G. Rowland, R. Bihrle, J.P. Donohue "Original
        Articles: Testis Cancer: Complications of Post-Chemotherapy Retroperitoneal
        Lymph Node Dissection" The Journal of Urology Volume 153, Issue 3,
        Supplement, March 1995, Pages 976–980

[13]   Alan W. Partin, MD, PhD; Michael W. Kattan, PhD; Eric N. P. Subong, MS;
        Patrick C. Walsh, MD; Kirk J. Wojno, MD; Joseph E. Oesterling, MD; Peter T.
        Scardino, MD; J. D. Pearson, PhD " Combination of Prostate-Specific Antigen,
        Clinical Stage, and Gleason Score to Predict Pathological Stage of Localized
        Prostate Cancer" JAMA. 1997;277(18):1445-1451.
        doi:10.1001/jama.1997.03540420041027.

[14]   Bockman DE, Büchler M, Beger HG. "Interaction of pancreatic ductal
        carcinoma with nerves leads to nerve damage." Gastroenterology. 1994
        Jul;107(1):219-30.

[15]   Mark Deakin, James Elder, Charles Hendrickkse, Daniel Peckham, David
        Leopard, Douglas A. Bell, Peter Jones, Hamish Duncan, Kate Brannigan, Julie
        Alldersea, Anthony A. Fryer and Richard C. Strange "SHORT
        COMMUNICATION: Glutathione S-transferase GSTT1 genotypes and
        susceptibility to cancer: studies of interactions with GSTM1 in lung, oral,

gastric and colorectal cancers" Oxford JournalsLife Sciences & Medicine Carcinogenesis Volume 17, Issue 4Pp. 881-884.

[16]   R. Hillenbrand, T. Taubner & F. Keilmann "Phonon-enhanced light–matter interaction at the nanometre scale" Nature 418, 159-162 (11 July 2002) | doi:10.1038/nature00899; Received 27 March 2002; Accepted 31 May 2002

[17]   Peter G. Shields and Curtis C. Harris "Cancer Risk and Low-Penetrance Susceptibility Genes in Gene-Environment Interactions" JCO June 11, 2000 vol. 18 no. 11 2309-2315

[18]   Marylyn D. Ritchie, Lance W. Hahn, Nady Roodi, L. Renee Bailey, William D. Dupont, Fritz F. Parl, Jason H. Moore "Multifactor-Dimensionality Reduction Reveals High-Order Interactions among Estrogen-Metabolism Genes in Sporadic Breast Cancer" Volume 69, Issue 1, July 2001, Pages 138–147

[19]   N. Ghosh, S. K. Mohanty, S. K. Majumder, and P. K. Gupta "Measurement of optical transport properties of normal and malignant human breast tissue" 2001 Optical Society of America

[20]   Elena Salomatina, Brian Jiang, John Novak, Anna N. Yaroslavsky " Optical properties of normal and cancerous human skin in the visible and near-infrared spectral range" Journal of Biomedical Optics 11(6), 064026 November/December 2006

[21]   Vivide Tuan-Chyan Chang, Peter S. Cartwright, Sarah M. Bean, Greg M. Palmer, Rex C. Bentley and Nirmala Ramanujam " Quantitative Physiology of the Precancerous Cervix In Vivo through Optical Spectroscopy" Volume 11 Number 4 April 2009 pp. 325–332 Neoplasia

[22]   Jie Wen, Tsutomu Arakawa, John S. Philo " Size-Exclusion Chromatography with On-Line Light-Scattering, Absorbance, and Refractive Index Detectors for Studying Proteins and Their Interactions" Analytical Biochemistry Volume 240, Issue 2, 5 September 1996, Pages 155–166

[23]   C L Arteaga, S D Hurd, A R Winnier, M D Johnson, B M Fendly, and J T Forbes " Anti-transforming growth factor (TGF)-beta antibodies inhibit breast cancer cell tumorigenicity and increase mouse spleen natural killer cell activity. Implications for a possible role of tumor cell/host TGF-beta

35

interactions in human breast cancer progression" J Clin Invest. 1993 December; 92(6): 2569–2576.

[24]   A. Roggan, D. Schädel, U. Netz, J.-P. Ritz, C.-T. Germer, G. Müller " The effect of preparation technique on the optical parameters of biological tissue" Appl. Phys. B 69, 445–453 (1999)

[25]   Dhiraj K. Sardar, Guang-Yin Swanland, Raylon M. Yow, Robert J. Thomas, Andrew T. C. Tsin "Optical properties of ocular tissues in the near infrared region " (2007) 22: 46–52

[26]   Scott Prahl " Everything I think you should know about Inverse Adding-Doubling " March 2011

[27]   en.wikipedia.org/ - Monochromator - 13.06.2013

[28]   J F Beeky, P Blokland, P Posthumus, M Aalders, J W Pickering, H J C M Sterenborg and M J C van Gemert "In vitro double-integrating-sphere optical properties of tissues between 630 and 1064 nm" Received 25 November 1996, in final form 10 July 1997

[29]   John W. Pickering, Scott A. Prahl, Niek van Wieringen, Johan F. Beek, Henricus J. C. M. Sterenborg, and Martin J. C. van Gemert "Double-integrating-sphere system for measuring the optical properties of tissue"

[30]   http://en.wikipedia.org/wiki/Lock-in_amplifier 27.05.2013

[31]   Sahimaa Abdelmonem, Mohammed Abdel Harith, Rehab Mohamed Amin, Aletta Karsten, Ann Singh " The Integrating sphere-based as an acurate system for optical properties measurements "

[32]   S. A. Prahl, M. J. C. van Gemert, and A. J. Welch, "Determining the optical properties of turbid media by using the adding-doubling method," Appl. Opt., vol. 32, pp. 559–568, 1993.

[33]   J. W. Pickering, S. A. Prahl, N. van Wieringen, J. F. Beek, H. J. C. M. Sterenborg, and M. J. C. van Gemert, "Double-integrating-sphere system for measuring the optical properties of tissue," Appl. Opt., vol. 32, pp. 399–410, 1993.

[34]   W. F. Cheong, S. A. Prahl, and A. J. Welch, "A review of the optical properties of biological tissues," IEEE J. Quantum Electron., vol. 26, pp. 2166–2185, 1990.

[35]   B. C. Wilson and G. Adam, "A Monte Carlo model for the absorption and flux distributions of light in tissue," Med. Phys., vol. 10, pp. 824–830, 1983. monte carlo.

[36]   G. N. Plass, G. W. Kattawar, and F. E. Catchings, "Matrix operator theory of radiative transfer. 1: Rayleigh scattering," Appl. Opt., vol. 12, pp. 314–329, 1973.

[37]   Sun Ying, Douglas S. Robinson, Qiu Meng, Luis T. Barata, Alan R. McEuen, Mark G. Buckley, Andrew F. Walls, Philip W. Askenase and A. Barry Kay "C-C Chemokines in Allergen-Induced Late-Phase Cutaneous Responses in Atopic Subjects: Association of Eotaxin with Early 6-Hour Eosinophils, and of Eotaxin-2 and Monocyte Chemoattractant Protein-4 with the Later 24-Hour Tissue Eosinophilia, and Relationship to Basophils and Other C-C Chemokines (Monocyte Chemoattractant Protein-3 and RANTES)" The Journal of Immunology October 1, 1999 vol. 163 no. 7 3976-3984

[38]   B Ardalan, L Chua, E M Tian, R Reddy, K Sridhar, P Benedetto, S Richman, A Legaspi, S Waldman and L Morrell "A phase II study of weekly 24-hour infusion with high-dose fluorouracil with leucovorin in colorectal carcinoma" JCO April 1991 vol. 9 no. 4 625-630

[39]   Angel, Michael F. M.D.; Ramasastry, Sai S. M.D.; Swartz, William M. M.D.; Narayanan, Krishna M.D.; Kuhns, Douglas B. Ph.D.; Basford, R. E. Ph.D.; Futrell, J. William M.D. "The Critical Relationship Between Free Radicals and Degrees of Ischemia: Evidence for Tissue Intolerance of Marginal Perfusion" Plastic & Reconstructive Surgery: February 1988

[40]   George Klein, Peter Clifford, Eva Klein, Richard T. Smith, Jun Minowada, François M. Kourilsky and Joseph H. Burchenal "Membrane Immunofluorescence Reactions of Burkitt Lymphoma Cells From Biopsy Specimens and Tissue Cultures" Oxford JournalsMedicine JNCI J Natl Cancer Inst Volume 39, Issue 5Pp. 1027-1044

[41] Gert-Jan Braunstahl, MDa, b, Shelley E. Overbeek, MD, PhDb, Alex KleinJan, BSca, Jan-Bas Prins, PhDb, Henk C. Hoogsteden, MD, PhDb, Wytske J. Fokkens, MD, PhDa "Nasal allergen provocation induces adhesion molecule expression and tissue eosinophilia in upper and lower airways" Journal of Allergy and Clinical Immunology Volume 107, Issue 3, March 2001, Pages 469–476

[42] Georg A. Bjarnason, Richard C.K. Jordan, Patricia A. Wood, Qi L, David W. Lincoln, Robert B. Sothern, William J.M. Hrushesky, Yaacov Ben-David "Circadian Expression of Clock Genes in Human Oral Mucosa and Skin : Association with Specific Cell-Cycle Phases" The American Journal of Pathology Volume 158, Issue 5, May 2001, Pages 1793–1801

[43] R. G. Giovanelli, "Reflection by semi-infinite diffusers," Optica Acta, vol. 2, pp. 153–162, 1955.

[44] David G. Goebel "Generalized Integrating-Sphere Theory" Applied Optics, Vol. 6, Issue 1, pp. 125-128 (1967)

[45] John W. Pickering, Christian J. M. Moes, H. J. C. M. Sterenborg, Scott A. Prahl, and Martin J. C. van Gemert "Two integrating spheres with an intervening scattering sample" Optics InfoBase - JOSA A - Volume 9 - Issue 4

[46] Leonard Hanssen "Integrating-Sphere System and Method for Absolute Measurement of Transmittance, Reflectance, and Absorptance of Specular Samples" Optics InfoBase - Applied Optics - Volume 40 - Issue 19

[47] F. J. J. Clarke, J. Anne Compton "Correction methods for integrating-sphere measurement of hemispherical reflectance" 13 MAR 2007 DOI: 10.1002/col.5080110406

[48] Blake G. Crowther "Computer modeling of integrating spheres" Optics InfoBase - Applied Optics - Volume 35 - Issue 30

[49] Y. Ohno "Integrating sphere simulation: application to total flux scale realization" Optics InfoBase - Applied Optics - Volume 33 - Issue 13

[50] Leonard M. Hanssen "Effects of restricting the detector field of view when using integrating spheres" Optics InfoBase - Applied Optics - Volume 28 - Issue 11

[51]   Greg McKee "Integrating Spheres Collecting and Uniformly Distributing Light" Labsphere, Inc

CURRICULUM VITAE

Name Surname: Volkan Dinç

Place and Date of Birth: İstanbul 02/04/1987

Address: Karslı Ahmet Cad. 4/16 Ataşehir İstanbul

E-Mail: dinc_volkan@hotmail.com

B.Sc.: İstanbul Kültür University – Faculty Of Arts & Science – Department Of Physix

Professional Experience:

Seven months of experience as a sales representative and almost one and a half year of experience as a clinical affairs director in orthopeadic market